P1

What Controls Wintertime Precipitation Distribution Across a Mountain Range? Insights from Regional Climate Simulations in the Interior Western US

Xiaoqin Jing, Bart Geerts and Yonggang Wang
University of Wyoming

AMS 17th Conference on Mountain Meteorology

UNIVERSITY OF WYOMING

Introduction: 10 years of 4 km WRF simulation

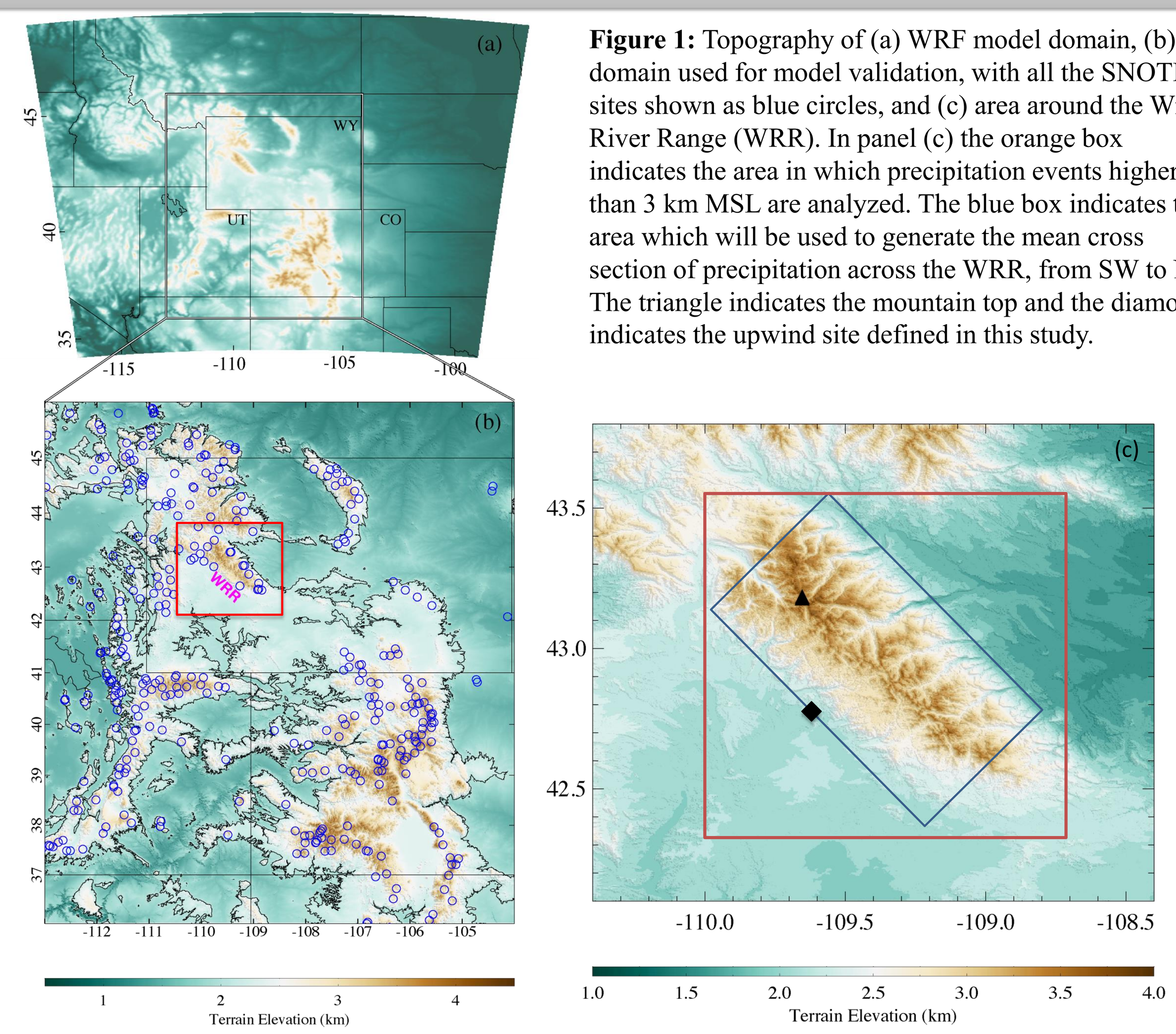

Figure 1: Topography of (a) WRF model domain, (b) domain used for model validation, with all the SNOTEL sites shown as blue circles, and (c) area around the Wind River Range (WRR). In panel (c) the orange box indicates the area in which precipitation events higher than 3 km MSL are analyzed. The blue box indicates the area which will be used to generate the mean cross section of precipitation across the WRR, from SW to NE. The triangle indicates the mountain top and the diamond indicates the upwind site defined in this study.

Motivation

- The distribution of precipitation across a mountain range is not well known, certainly not for individual storms, because of the paucity of gauges, the uncertainty of gauge-base measurements of snowfall, and the challenges of radar-based orographic precipitation estimation.
- High-resolution NWP simulations can yield insights into orographic precipitation distribution, and factors controlling it.

WRF model configuration

- 420x410 grid points, 51 vertical levels;
- single domain, 4 km grid spacing;
- NOAH-MP land surface model;
- RRTMG radiative transfer scheme;
- Thompson microphysics scheme;
- convection resolving;
- YSU PBL scheme;
- driven by CFSR.

Model validation datasets

PRISM
- Statistical model based on precipitation-terrain relation;
- Based on SNOTEL network over mountains (and other gauge networks elsewhere);
- Daily/monthly data at 4 km x 4km;

SNOTEL
- Point gauge data in mountains;
- Daily precipitation;

NCEP IV
- Combined ground-based scanning radar and gauge data;
- Hourly data at 4 km x 4km;

WRF is run continuously for 10 years (March 2002 to February 2012). Here we use wintertime data only (DJF).

How good is WRF? Comparison with observations over mountains in the Interior West

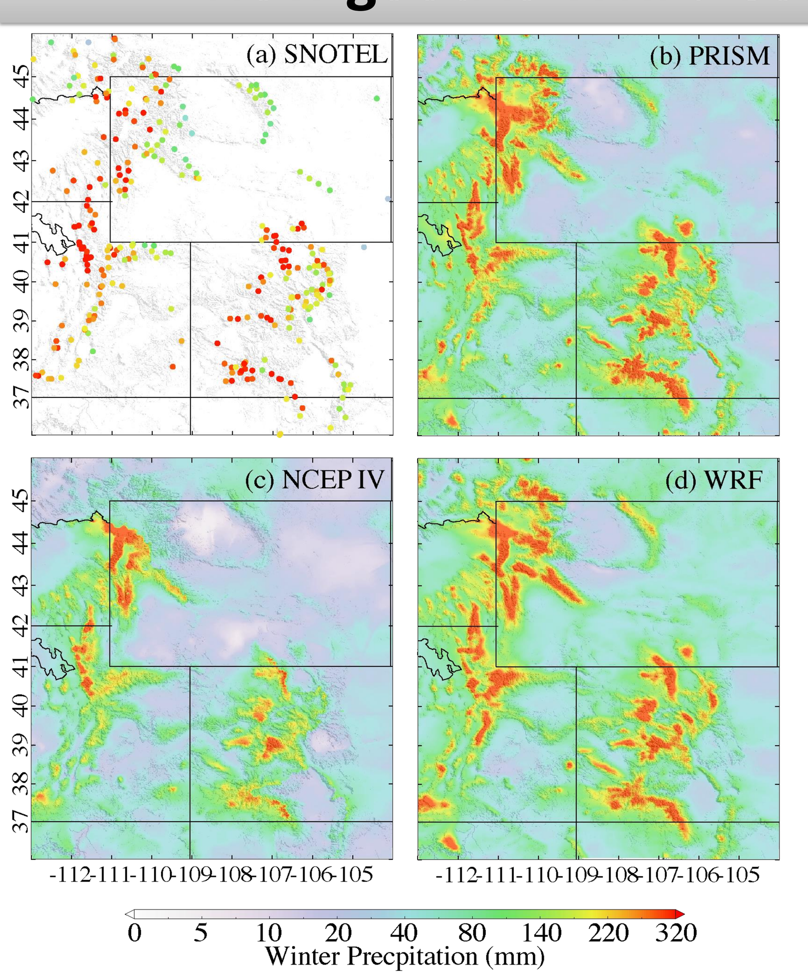

Figure 2: Mean winter precipitation (total over 3 months, DJF) maps in the interior western US estimated by SNOTEL, PRISM, NCEP IV and WRF.

- PRISM is quite consistent with SNOTEL over mountain areas (as expected), while NCEP IV grossly underestimates winter precipitation over mountains (Fig. 2).
- WRF appears to capture winter precipitation amounts and distribution in mountain areas: at most of the SNOTEL sites, the mean monthly difference is less than 20 mm/month (generally less than 10%) in DJF, and the correlation coefficient based on monthly data is greater than 0.9 (Fig. 3).
- Neither the bias nor the correlation coefficient clearly relates with terrain elevation (Fig. 3b, d)
- *Therefore we can use the 10 year WRF simulation to study precipitation distribution across a mountain range.*
- Here we focus on the Wind River Range in Wyoming.

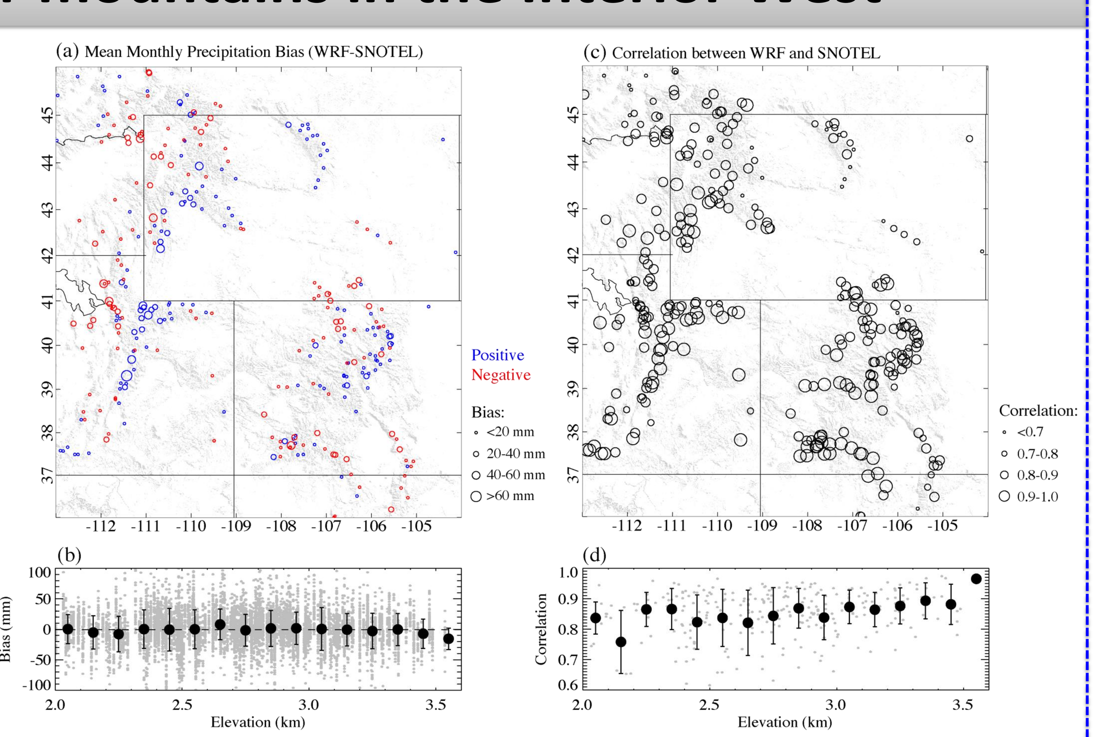

Figure 3: (a) Mean monthly precipitation bias in winter (DJF) between WRF and SNOTEL (WRF-SNOTEL) (mm/month). (b) Monthly precipitation bias in winter between WRF and SNOTEL as a function of elevation. The gray dots indicate the monthly precipitation bias at all the SNOTEL sites in winter between March 2002 and February 2012. The black dots are the mean values at different elevation intervals and the black bars indicate one standard deviation. (c) and (d) are similar to (a) and (b) but for correlation coefficients between WRF and SNOTEL.

PDFs of ambient conditions during winter storms over the Wind River Range

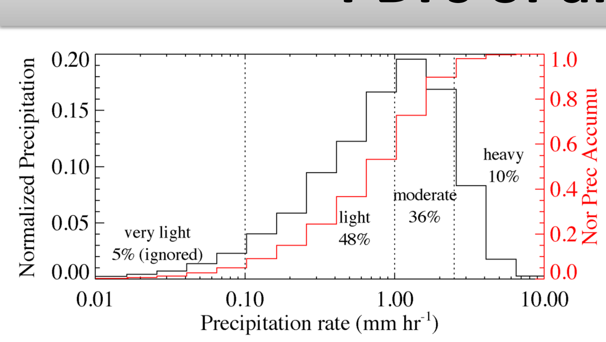

Figure 4: Histogram of normalized precipitation and precipitation accumulation as function of precipitation rate. The relative contributions from very light, light, moderate and heavy precipitation events to the total precipitation are shown.

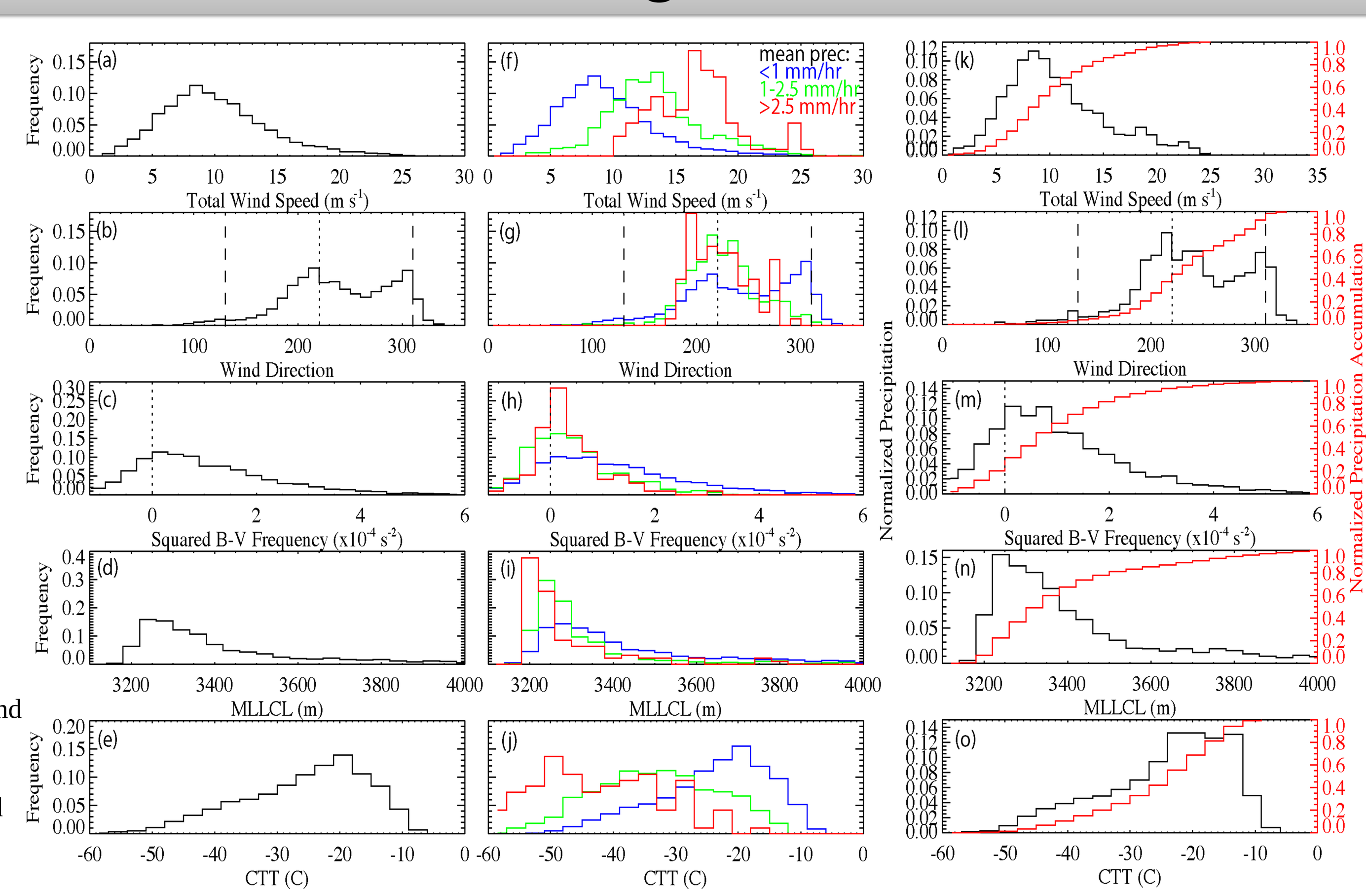

Figure 5: Normalized PDFs of total wind speed, wind direction, N^2, MLLCL and CTT for (a-e) all precip events and (f-j) cases with different mean precip rate above 3 km MSL. (k-o) Normalized precip and precip accumulation as functions of wind speed, wind direction, N^2, MLLCL and CTT. The dotted line in (b), (g) and (l) indicate the wind direction normal to WRR (SW to NE). The dashed lines in the same panels indicate the orientation of WRR (130° to 310°).

Definitions

- The data base is hourly WRF data over 30 winter months (DJF, 10 years). A precip event is defined as any hour having mean precip rate >0.1 mm/hr above 3 km MSL in the WRR (orange box in Fig. 1c). There are 5113 precip events in total.
- Wind speed and wind direction are averaged from surface to mountain top height at the upwind site (diamond in Fig. 1c), at the beginning of the 1-hr precip event (time t_o).
- B-V frequency N is the average of dry N below MLLCL and moist N from MLLCL to mountain top at the upwind site, at time t_o.
- MLLCL is calculated using the mean temperature and dew point temperature of the lowest 50mb levels of the atmosphere, at time t_o.
- CTT is averaged for the grid points where cloud exists and where P>0 over the WRR. A cloud is defined as having total condensed water mixing ratio grater than 0.01 g m^{-3}.

Findings

- Heavy precip arises from deep systems (low cloud base, high cloud top) & strong cross-barrier winds, light precip from shallow systems & lighter winds.
- Moderate to heavy precip is mostly orographic (cross-barrier flow). The wind direction during light precip is bimodally distributed (cross-mountain and along-mountain). A SE barrier jet is very uncommon.
- Both stable (stratiform) and unstable (convective) events occur.

Precipitation distribution at WRR with different ambient conditions

--------- Wind Speed Dependent Precipitation Distribution ----------

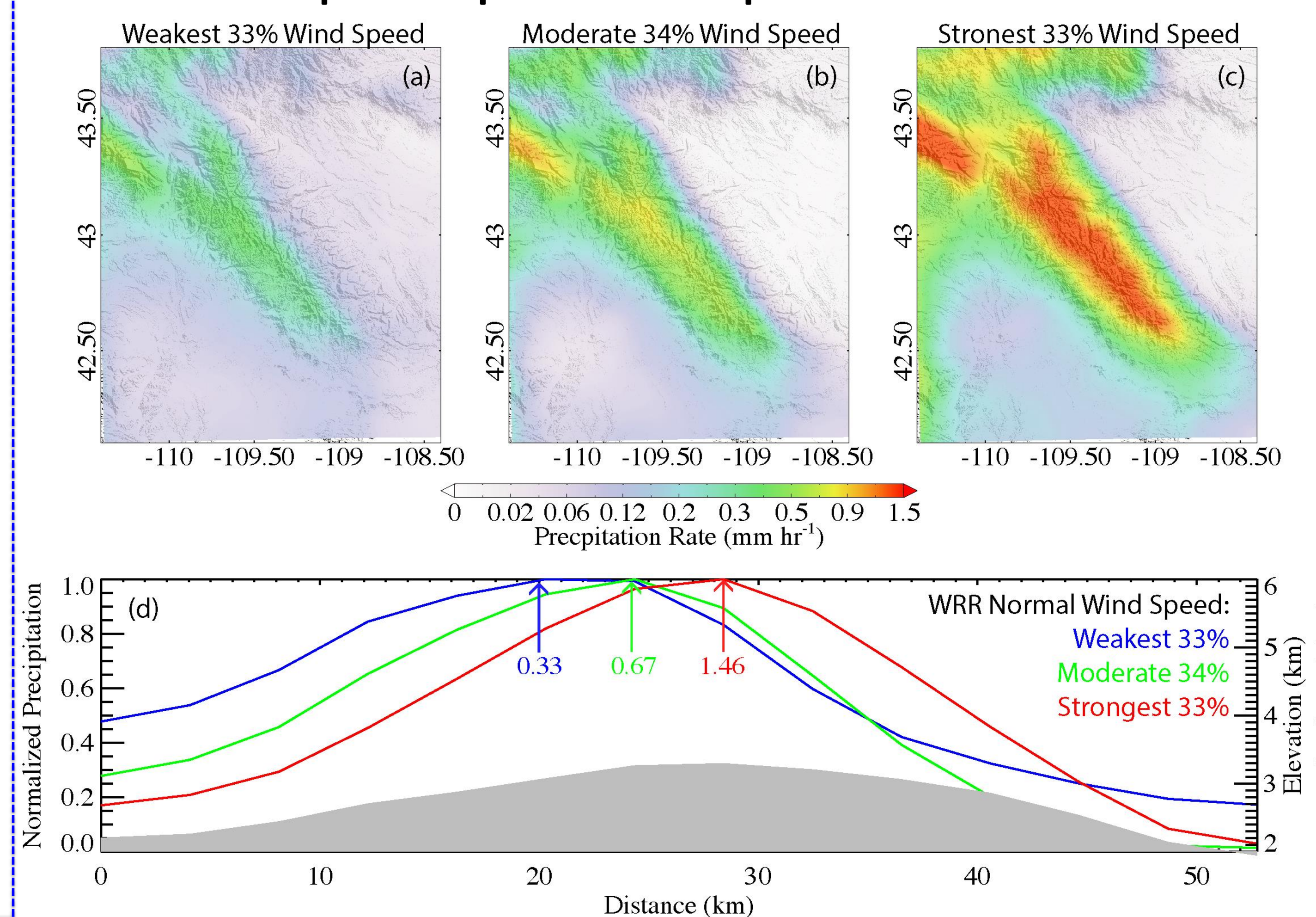

Figure 6: (a-c) Maps of mean precipitation distribution at WRR for cases with the weakest 33%, moderate 34% and strongest 33% mountain-normal wind speed. (d) Mean normalized precipitation across WRR from SW to NE (computed over the blue box in Fig. 1c). The location and amount of max. precip rate (mm/hr) for each mean cross sections are shown.

--------- Stability Dependent Precipitation Distribution ----------

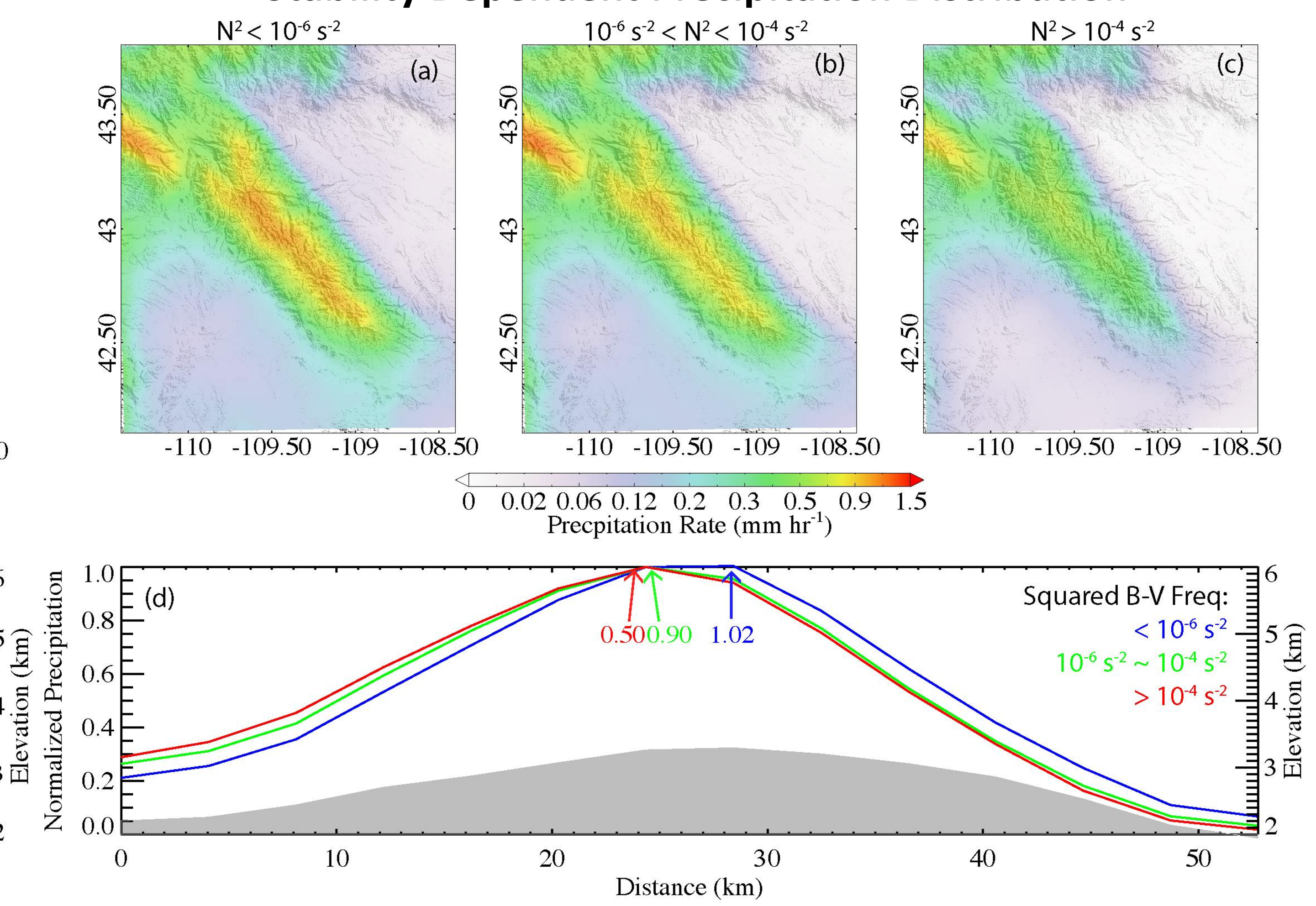

Figure 7: Similar to Fig. 6 but for B-V frequency N^2. The three groups shown represent (a) 17% (unstable), 46% (weakly stable), and 37% (highly stable) of all precip events.

-------- Mixed-Layer LCL Dependent Precipitation Distribution --------

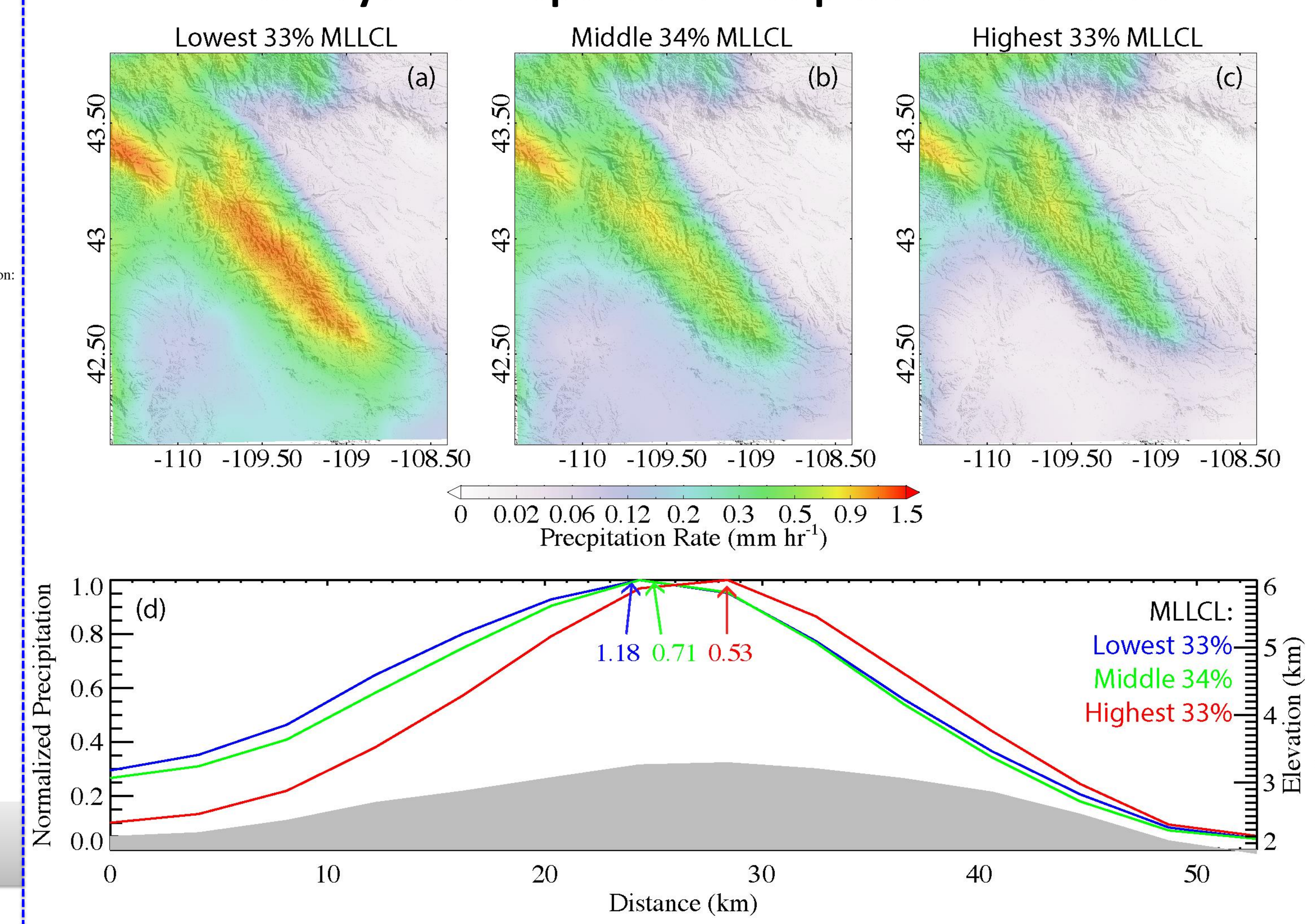

Figure 8: Similar to Fig. 6 but for mixed-layer LCL.

--------- CTT Dependent Precipitation Distribution ----------

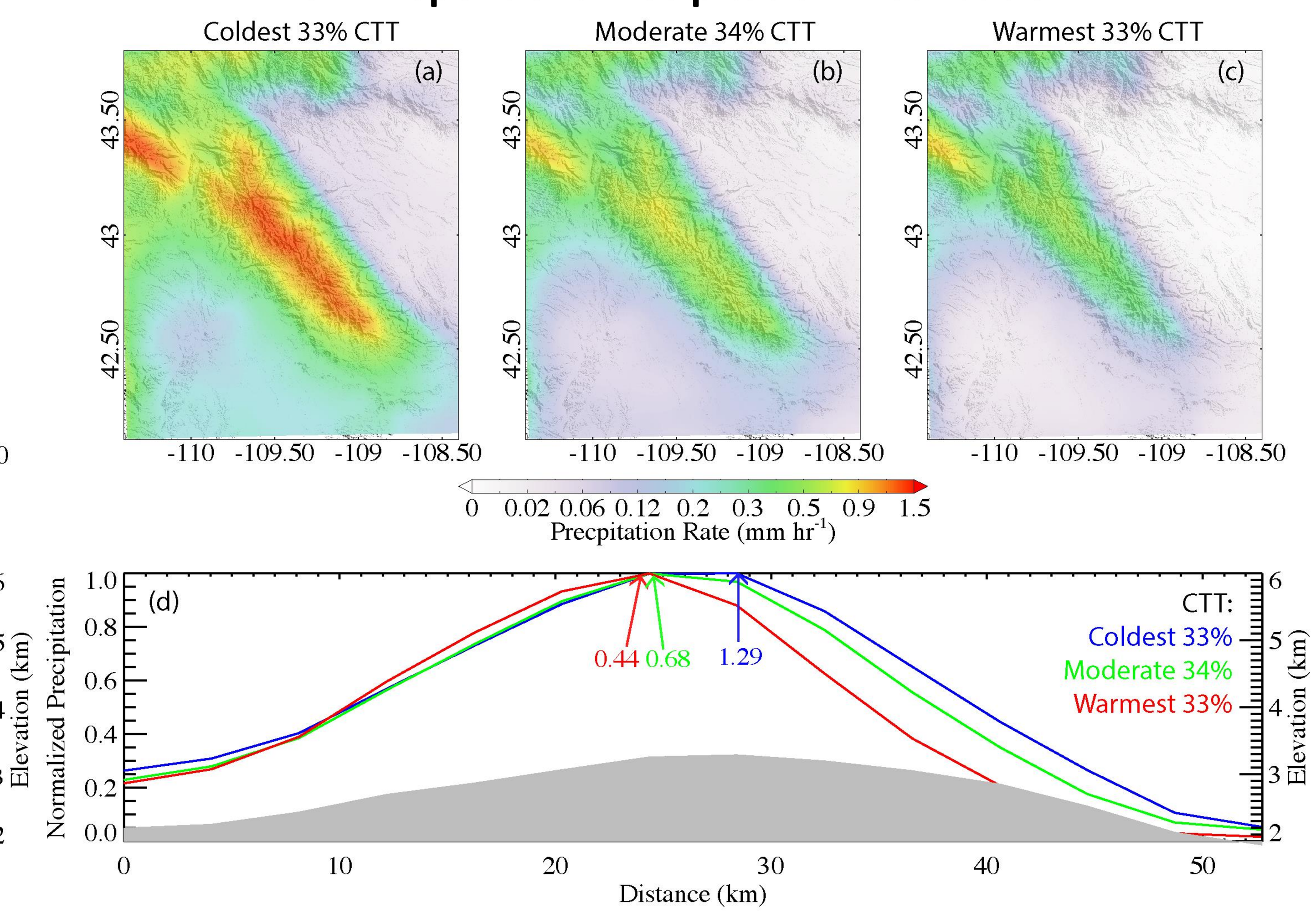

Figure 9: Similar to Fig. 6 but for squared cloud top temperature.

Findings (Fig. 6-9):

- Here only precip events with cross-barrier flow from the SW (wind directions from 180 to 270°) are considered. They comprise the bulk of all precip events (Fig. 5b), 4013 in total.
- Heavier precip occurs under stronger cross-barrier wind, lower stability (convection), lower LCL and lower CTT (higher cloud top).
- Most precip falls on the upwind side near the crest, with rapid drying in the lee. Stronger wind, lower stability (convection), higher LCL and deeper cloud result in relatively more precip on the lee side. Wind speed is the main driver for leeside precip enhancement.

Conclusions

- Following a series of sensitivity tests, we identified a configuration of WRF that simulates wintertime precip very well over mountains in the interior West, according to SNOTEL estimates for a 10 year period. This configuration includes the Thompson microphysics scheme and a 4 km, 51 layer resolution.
- Given this performance, the simulation can be used to examine the distribution of precipitation across mountain ranges in the interior West, at spatial and time scales much finer than available observationally. Here we focus on the Wind River Range in Wyoming.
- Winter precip distribution across a mountain range is strongly affected by ambient conditions. Statistically, heavier precipitation is associated with stronger wind, lower stability (convection), greater storm depth (lower cloud base and colder cloud tops). The same first two factors, as well as higher cloud (higher base and top), also yield relatively more precipitation on the lee side.

Acknowledgement: This work is supported by the University of Wyoming's Office of Water Program.